ARTICLE
Journal of Cellular Biochemistry 114:2677–2689 (2013)

Journal of Cellular Biochemistry

Migration of CXCR4 Gene-Modified Bone Marrow-Derived Mesenchymal Stem Cells to the Acute Injured Kidney

Nanmei Liu,* Jun Tian, Jin Cheng, and Jinyuan Zhang

Department of Nephrology, The 455th Hospital of PLA, Shanghai, 200052, China

ABSTRACT

Bone marrow-derived mesenchymal stem cells (BMSCs) can migrate to the injured kidney after acute kidney injury (AKI) with limited efficiency. This study investigated the effect of CXCR4 overexpression on BMSC migration to the AKI kidney and the possible mechanisms. CXCR4 gene-modified BMSCs (CXCR4-BMSCs) and null-BMSCs were prepared and transplanted into the AKI mice. Blood indicators, histology, expression of stromal cell-derived factor 1 (SDF-1), and BMSC migration were investigated. Hypoxia/re-oxygenation-pretreated renal tubular epithelial cells (HR-RTECs) were prepared to generate AKI in vitro. The chemotaxis experiment was performed using the transwell chamber. The phosphorylation of AKT and MAPK in the BMSCs was also investigated. The CXCR4-BMSCs showed a remarkable expression of CXCR4. The SDF-1 expression in the AKI renal tissue was increased. CXCR4-BMSCs transplantation sharply increased the accumulation of BMSCs in the renal tissue, which was consistent with a greater improvement of renal function. The in vitro experiments showed that the migration of BMSCs to the HR-RTEC culturing chamber was CXCR4-dependent, and could be fully inhibited by AMD3100, a CXCR4-specific antagonist. The migration could also be partly blocked by either LY294002 (PI3K inhibitor) or PD98059 (MAPK inhibitor). Phosphorylated Akt and MAPK were increased in the BMSCs co-cultured with HR-RTECs and their expression was the highest in the CXCR4-BMSCs, which could be recovered by AMD3100. *Overexpression of* CXCR4 gene could enhance BMSC migration to the kidney area after AKI. The SDF-1/CXCR4 axis via its activation of PI3K/AKT and MAPK in BMSCs could be the possible mechanisms underlying this function. J. Cell. Biochem. 114: 2677–2689, 2013.

KEY WORDS: MIGRATION; CXCR4; BONE MARROW-DERIVED MESENCHYMAL STEM CELLS; ACUTE KIDNEY INJURY; HYPOXIA/RE-OXYGENATION; RENAL TUBULAR EPITHELIAL CELLS

Acute kidney injury (AKI) is a commonly occurring clinical disease and relevant therapies are being developed. However, its prognosis and mortality are still significant issues. Apoptosis of the renal tubular epithelial cells (RTECs) is the main pathological manifestation of AKI. The bone marrow-derived mesenchymal stem cells (BMSCs) applied in vitro and in vivo can be differentiated into functional RTECs [Herrera et al., 2004; Morigi et al., 2004; Liu et al., 2011]. In addition, the para- and endocrine actions of BMSCs also facilitate the self-repair of the injured RTECs [Semedo et al., 2007; Eliopoulos et al., 2010; Gatti et al., 2011]. Therefore, BMSC transplantation has become a promising candidate for multiple cell-based therapies of AKI. However, it has been suggested that the repair efficiency is limited [Stolzing and Scutt, 2006; Hoffmann et al., 2010]. The main reason could be that only a small proportion of the implanted BMSCs migrate to the injured kidney and play the role there.

After BMSC transplantation, the transplanted cells can reach the injured tissue via blood circulation, but a large number of cells still stay in other blood-rich organs, for example, lung, liver, and spleen. Therefore, to increase the repair efficiency when only a limited number of BMSCs are transplanted, it is vital to improve the migration of BMSCs to the injured kidney. Stromal cell-derived factor-1 (SDF-1) and its cellular receptor, CXCR4, have been demonstrated to direct the migration of stem cells associated with injury repair in many species and tissue types [Floridi et al., 2003; Yamaguchi et al., 2003; Tögel et al., 2005]. The expression of SDF-1 is

Grant sponsor: Shanghai Rising-star Program; Grant number: 12QA1405000; Grant sponsor: Shanghai Municipal Natural Science Foundation; Grant number: 11ZR1449600; Grant sponsor: Shanghai Key Projects of Basic Research; Grant number: 12DJ1400203.

*Correspondence to: Nanmei Liu, Department of Nephrology, The 455th Hospital of PLA, Shanghai 200052, China
E-mail: liunanmei@gmail.com

Manuscript Received: 27 March 2013; Manuscript Accepted: 14 June 2013
Accepted manuscript online in Wiley Online Library (wileyonlinelibrary.com): 24 June 2013
DOI 10.1002/jcb.24615 • © 2013 Wiley Periodicals, Inc.

predominantly promoted under the ischemia conditions including AKI [Askari et al., 2003; Tögel et al., 2005; Shen et al., 2007; Lai et al., 2008; Li et al., 2009]; however, the expression of CXCR4 on the surface of BMSCs is not high [Wang et al., 2008]. Hence, the enhancement of CXCR4 expression on BMSCs should be able to increase the directional migration and the injury repair efficiency of BMSCs.

In this study, we enhanced the CXCR4 expression on BMSCs using the gene transfection technique. We monitored the migration of CXCR4 gene-modified BMSCs (CXCR4-BMSCs) to the kidney area in response to AKI and the corresponding treatment effect in the AKI mouse models. The possible mechanisms were also explored.

MATERIALS AND METHODS

CONSTRUCTION OF CXCR4-BMSCs CARRYING BOTH CXCR4 AND eGFP GENES AND NULL-BMSCs CARRYING ONLY THE eGFP GENE

Plasmid construction using gateway technology. PCR amplification of attB1-CXCR4-attB2 (or attB1-eGFP-attB2): PCR was performed in 50 μl mixture containing 0.5 μl of Primer STAR™ HS DNA Polymerase (Takara Bio, Inc., Otsu, Japan), 10 μl of 5× Primer STAR™ buffer (Mg^{2+} Plus), 4 μl of dNTP mixture (10 μM, Fermentas, USA), 1 μl of primer-F (10 μM, sequence listed in Table I), 1 μl of primer-R (10 μM, sequence listed in Table I), and 1 μl of template DNA. The mixture was heated to 98°C for 3 min followed by an additional 30 PCR cycles (98°C for 10 s, 60°C for 10 s, and 72°C for 60 s per cycle). The amplified attB1-CXCR4-attB2 (or attB1-eGFP-attB2) fragment was incubated at 72°C for 5 min to form the final PCR products, which were then purified using the QIAquick Gel Extraction Kit (Qiagen, Valencia, CA).

The amplified attB1-CXCR4-attB2 (or attB1-eGFP-attB2) was then inserted into the gateway entry vector pDONR221 (Cyagen Biosciences, Inc, Guangzhou, China) using the BP Clonase™ II Enzyme Mix (Invitrogen, Carlsbad, CA). Two microliters of BP products was added into the vial containing One Shot® stb13™ chemically competent cells *Escherichia coli* (Invitrogen) according to the manufacturer's protocol. Positive clones of pDown-CXCR4 (or pDown-eGFP) were screened using Colony PCR. An LR integration reaction combining the pDown-CXCR4 (or pDown-eGFP) and the destination vector pLV.Des3d.P/puro (or pLV.Des2d.P/Neo) was performed using the LR Clonase™ II Enzyme Mix (Invitrogen). Products from the LR reaction were directly used for bacterial transformation and Colony PCR was performed to screen the target plasmids, that is, pLV.EX3d.P/puro-CMV > CXCR4 > IRES/eGFP *and* pLV.EX2d.P/Neo-CMV > eGFP. Here, pLV.EX2d.P/Neo-CMV > eGFP was constructed as the control.

Lentivirus packaging. To generate the virus encoding the lenti-CXCR4-eGFP/puro (or lenti-eGFP/neo), pLV.EX3d.P/puro-CMV > CXCR4 > IRES/eGFP (or pLV.EX2d.P/Neo-CMV > eGFP) together with pLV/helper-SL3, pLV/helper-SL4, and pLV/helper-SL5 were co-transfected into 293FT cells (SIBCB, CAS, China) using lipofectamine 2000 (Invitrogen) according to the manufacturer's instructions. The culture medium supernatant containing the lentivirus particles was harvested and ultra-centrifuged. Virus titer was determined via crystal purple staining.

BMSC infection and selection. Mouse P3 BMSCs (ATCC, Manassas, VA) were seeded in 6-well plates. When the cell confluence reached 60–80%, the culture medium was replaced by the appropriately titered viral supernatant (lenti-CXCR4-eGFP/puro or lenti-eGFP/neo, 1.5 ml/well) and the cells were incubated at 37°C for 16 h. Afterwards, the viral supernatant was replaced by fresh BMSC complete culture medium (Sciencell Research Labs, CA, USA). Forty-eight hours later, the infected cell populations were selected in the 500 μg/ml puromycin (or neomycin) and the medium was changed every 2 days. Selection was terminated when the blank cells were completely dead and the antibiotic free medium was used for propagation. The eGFP-positive cells under the fluorescence microscope represent the infected BMSCs. Both the CXCR4-BMSCs (carrying CXCR4 and eGFP genes) and the null-BMSCs (only carrying the eGFP gene) were prepared for further use.

CHARACTERIZATIONS OF CXCR4-BMSCs AND NULL-BMSCs

CXCR4 levels in the transfected BMSCs. Reverse transcription-PCR (RT-PCR) method was performed to determine the mRNA level of CXCR4 in CXCR4-BMSCs and null-BMSCs. Sequences of the PCR primers are listed in Table II.

The protein expression of CXCR4 was determined by Western blot. CXCR4-BMSCs and null-BMSCs were scraped in RIPA lysis buffer containing protease inhibitors. After sodium dodecyl sulfate–polyacrylamide gel electrophoresis (SDS–PAGE), the protein was transferred to a PVDF membrane and blocked with TBST containing 1% BSA (10 mM Tris–HCl, pH 7.14, 150 mM NaCl, 1% Tween-20) at room temperature for 4 h. The PVDF membrane was incubated with rabbit anti-mouse CXCR4 monoclonal antibody (Biosynthesis Biotechology Co., LTD, Beijing, China) at 4°C overnight. HRP labeled goat anti-rabbit IgG (Santa Cruz Biotechnology, Inc., CA, USA) was added and incubated for another hour at room temperature. The mixture of reacted ECL was added onto the PVDF membrane for 1–2 min, which was then placed on a Fiuorchem HD2 gel image analysis system for observation. The gray value of the band was measured.

TABLE I. Primers Used in PCR Amplification of attB1-CXCR4-attB2 and attB1-eGFP-attB2

Primers	Oligo sequence (from 5′ to 3′)
CXCR4	
attB1-Kozak-CXCR4	GGGGACAAGTTTGTACAAAAAAGCAGGCTGCCACCATGGAACCGATCAGTGTGAGT
attB2- CXCR4	GGGGACCACTTTGTACAAGAAAGCTGGGTTTAGCTGGAGTGAAAACTGGAG
eGFP	
attB1-Kozak-eGFP	GGGGACAAGTTTGTACAAAAAAGCAGGCTGCCACCATGGTGAGCAAGGGCGAGG
attB2-eGFP	GGGGACCACTTTGTACAAGAAAGCTGGGTTTACTTGTACAGCTCGTCCATG

TABLE II. Primers Used for RT-PCR of CXCR4

Gene	Forward primer	Reverse primer
CXCR4	5′ATGGAACCGATCAGTGTGAGT3′	5′TTAGCTGGAGTGAAAACTGGAG3′
GAPDH	5′CAAGGTCATCCATGACAACTTTG3′	5′GTCCACCACCCTGTTGCTGTAG3′

GAPDH was used as the internal reference. The protein expression was represented as the ratio of the band gray value of CXCR4 to that of GAPDH.

For assessment of expression of CXCR4 on the cell surface, cultured CXCR4-BMSCs and null-BMSCs were incubated with an Alexa Fluor 647 anti-mouse CD184 (CXCR4) or an isotype-matched control (Alexa Fluor 647 Rat IgG2b, κ Isotype Ctrl; both were purchased from Biolegend, San Diego, CA) in the dark room at 4°C for 30 min. Flow cytometric analysis was performed using the MACS Quant flow cytometer (Miltenyi Biotech, Bergisch Gladbach, Germany).

Surface marker. CXCR4-BMSCs and null-BMSCs were harvested and incubated with a phycoerythrin (PE)-conjugated anti-CD44 antibody, a fluorescein isothiocyanate (FITC)-conjugated anti-CD45 antibody or an isotype-matched control (all were purchased from BD Biosciences, CA, USA) in the dark room. Flow cytometric analysis of the cell surface CD44 and CD45 was performed using the BD Biosciences flow cytometer.

Mesenchymal differentiation. *Osteogenic induction detection.* CXCR4-BMSCs and null-BMSCs were incubated in the osteogenic induction medium (Cyagen Biosciences, Inc., Guangzhou, China) for 21 days. After washing with PBS, the cells were fixed with 4% paraformaldehyde for 30 min. Alizarin red was added for 5 min staining followed by cleaning, and the cells were observed under the microscope.

Detection of chondrogenic induction. CXCR4-BMSC and null-BMSC suspensions were added into the polypropylene culture tubes and cultured with complete chondrogenic induction medium (Cyagen Biosciences, Inc.) for 21 days after centrifugation. The harvested chondrogenic pellets were formalin-fixed and paraffin-embedded. Alcian blue solution was added for 30 min staining followed by cleaning, and the cells were observed under the microscope.

Adipogenic induction detection. After incubation in the adipogenic induction medium (Cyagen Biosciences, Inc.) for 18 days, the cells were fixed with 4% paraformaldehyde for 30 min. Oil red O was added for 10 min staining followed by cleaning, and the cells were observed under the microscope.

Cell viability. CXCR4-BMSCs, null-BMSCs and BMSCs were all seeded in 96-well plates at a density of 2×10^3/well, and cultured with BMSC complete culture medium for 1, 2, 3, 4, 5, 6, and 7 days, respectively. The MTT method was employed to measure the cell proliferation.

AKI MOUSE MODEL PREPARATION, EXPERIMENTAL GROUPING, AND SETTLEMENT

In order to detect the accumulation of BMSCs to the injured kidney, mouse BMSCs, CXCR4-BMSCs, and null-BMSCs were all labeled with bromodeoxyuridine (BrdU) by culturing them with low-glucose DMEM (Invitrogen) containing 10 μM BrdU (Sigma–Aldrich, St. Louis, MO, USA) for 72 h, and the labeling efficiency was determined by the proportion of BrdU-positive BMSCs (BrdU-BMSCs), using the immunohistochemistry (IHC) method. C57BL/6 mice (Experimental Animal Center of the Second Military Medical University, 20 ± 2 g) were used to develop the AKI model by clamping the bilateral renal pedicles for 30 min and reopening for 30 min. The mice were randomly divided into the following groups: the normal group (sham group), the model group, the BMSCs group (2×10^6 BrdU-BMSCs were transplanted into the AKI mice via tail vein), the null-BMSCs group (2×10^6 BrdU-null-BMSCs were transplanted into the AKI mice via tail vein) and the CXCR4-BMSCs group (2×10^6 BrdU-CXCR4-BMSCs were transplanted into the AKI mice via tail vein). All mice were fed at a favorable temperature and humidity with an unlimited supply of water and food. For each group, five mice were sacrificed at 1, 3, 7, and 14 days after transplantation, respectively. Blood samples were collected and the serum was isolated and stored at −20°C. After perfusion with PBS via the heart, the bilateral kidneys were separated and further perfused with PBS. The corticomedullary junction of the kidneys was cut and fixed with 10% formalin for pathological and IHC analysis. All procedures were performed in accordance with the principles of the Guidelines for Animal Experimentation of the Second Military Medical University (Shanghai, China).

SDF-1 LEVEL IN THE RENAL TISSUE

The samples were treated with 1 ml of lysis buffer and centrifuged at 20,000 rpm (4°C) for 10 min. The supernatant was centrifuged for another 10 min at 12,000 rpm (4°C). The protein concentration was measured. Western blot analysis was used according to the protocols described above with the rabbit anti-mouse SDF-1 monoclonal antibody (Abcam, Inc., Cambridge, UK). β-Actin was used as the internal reference and the protein expression was the ratio of band gray value of SDF-1 to that of β-actin.

ASSESSMENT OF BMSC MIGRATION IN VIVO

The IHC method was employed. The paraffin sections were de-waxed with dimethylbenzene and dehydrated with graded ethanol. After blocking endogenous peroxidase with 0.3% H_2O_2, the sections were placed in a container filled with citrate buffer. After adding the antigen restored liquid, the container was heated to 98°C for 3 min to expose the antigen. The sections were incubated with the BrdU monoclonal antibody (Sigma–Aldrich) at 4°C for 16 h. After washing with PBS, the sections were incubated with the HRP labeled anti-mouse lgG (Santa Cruz, Inc., CA, USA) at 37°C for 1 h. Then the sections were incubated in the DAB chromogenic substrate liquid for 15 min, and lining was stained with hematoxylin. After being sealed with resin, the sections were stored at room temperature for use. Fifteen non-overlapping view fields (200×) were chosen for each section to determine the proportion of $BrdU^+$ cells (BMSCs) in the corticomedullary junction of the kidneys. The mean value of the proportion of $BrdU^+$ cells for each section was used for the statistical analysis.

BLOOD BIOCHEMICAL INDICATORS

The concentrations of blood urea nitrogen (BUN) and serum creatinine (Scr) were measured using the Beckman Automatic Biochemistry Analyzer (Beckman Coulter, Inc.).

PATHOLOGICAL CHANGES

The fixed samples were used to make paraffin sections. After HE staining, the degree of tubular necrosis was scored using the blinding method. Briefly, for each section, 15 view fields were chosen under the 200× magnification for scoring: 0 = normal, 1 = minor injury (injured tubular <5%), 2 = mild injury (injured tubular 5–25%), 3 = medium injury (injured tubular 25–75%), and 4 = severe injury (injured tubular >75%). Semi-quantitative analysis was performed and the mean score value was used to indicate the degree of acute tubular necrosis (ATN scoring).

A HYPOXIA/RE-OXYGENATION (HR) MODEL OF RTECs TO GENERATE AKI IN VITRO

Based on our preliminary experiment, the HR model of RTECs (HR-RTECs) was prepared: 4×10^5 cells/well of mouse RTECs (ATCC) were seeded in 6-well plates and cultured under the hypoxia condition (3% O_2, 5% CO_2, and 92% N_2) using the AnaeroPack™ System (Mitsubishi Gas Chemical Co., Inc., Tokyo, Japan) with glucose-free DMEM (Invitrogen) for 12 h. Then they were cultured under the re-oxygenation condition (95% air and 5% CO_2) with low-glucose DMEM for an additional 12 h. These HR-RTECs were used to generate AKI in vitro. Normoxia-preconditioned (for 24 h in 95% air, 5% CO_2) RTECs in the 6-well plates were used as the control.

SDF-1 LEVELS IN RTECs AND HR-RTECs

Protein expression. Cell lysate was added into the 6-well plates for full lysis of RTECs (or HR-RTECs). The supernatant was removed after centrifugation and the protein concentration was measured. Western blot was employed as described above with the rabbit anti-mouse SDF-1 monoclonal antibody as the primary antibody. β-Actin was used as the internal reference. The protein expression was represented by the ratio of the band gray value of SDF-1 to that of β-actin.

Supernatant concentration. The RTEC and HR-RTEC culture medium supernatant in the 6-well plates were collected to measure the concentration of SDF-1 according to the instructions of the SDF-1 enzyme-linked immunosorbent assay (ELISA) Detection Kit (Round Record Biotech Co., Ltd, Shanghai, China).

CHEMOTAXIS ASSAY IN VITRO

The chemotaxis experiment was conducted using the transwell chamber with an 8-μm pore size polycarbonate filter (Coring Incorporated, NY, USA). Upon completion of the preparations of HR-RTECs and control RTECs, the 6-well plates with HR-RTECs or RTECs were removed from the incubator and the transwell chambers were inserted into the plates. Mouse BMSCs, CXCR4-BMSCs, and null-BMSCs resuspended in the medium were placed in the upper chambers. The plating density was 1.8×10^5 cells/chamber. The chemotaxis assay was used for the following groups: the B/R group (BMSCs/RTECs), the B/H group (BMSCs/HR-RTECs), the C/H group (CXCR4-BMSCs/HR-RTECs), and the N/H group (null-BMSCs/HR-RTECs). For the inhibition experiments, mouse CXCR4-BMSCs were pre-incubated with 5 mg/ml AMD3100 (CXCR4-specific antagonist), 20 μM LY294002 (phosphoinositide 3-kinase (PI3K) inhibitor), 5 μM PD98059 (MAPK inhibitor; all were purchased from Sigma–Aldrich) and 20 μM LY294002 + 5 μM PD98059, respectively, for 30 min, and then were added into the upper chamber. All groups were incubated at 37°C for 12 h in a humidified atmosphere with 5% CO_2. Upon completion of the incubation, the nonmigrating BMSCs from the upper surface of the polycarbonate membrane were wiped-off with a cotton bud. The BMSCs under the membrane were stabilized with 4% paraformaldehyde for 20 min and stained with 1% crystal violet for 30 min. In the final step, PBS cleaning was carried out till the violet color became dim. Photographs were taken for each membrane under the microscope, the number of cells in five non-overlapped view fields was counted, and the average number of migrating cells was calculated.

PHOSPHORYLATION OF AKT AND MAPK IN BMSCs

After completion of the co-culturing, the transwell chambers were transferred to the new blank 6-well plates and cell lysate was added for full lysis of the BMSCs. Western blot was used as described above with the rabbit anti-mouse phospho-Akt (pAKT) and phospho-MAPK (pMAPK) monoclonal antibodies (both were purchased from CST, Inc., MA, USA) as the primary antibodies. GAPDH was used as the internal reference and the protein expression was represented as the ratio of the band gray values of pAKT or pMAPK to that of GAPDH.

STATISTICAL ANALYSIS

The results were expressed as means ± standard deviation (SD). Student's *t*-test was performed to analyze the differences between the two groups. Multiple-group comparison was performed using one-way analysis of variance (ANOVA) followed by a Student–Newman–Keuls test. SPSS17.0 statistical software was used for the analysis. Values of $P < 0.05$ were considered statistically significant.

RESULTS

PLASMID CONSTRUCTION, LENTIVIRUS PACKAGING, AND BMSC INFECTION

By gateway technology, pLV.EX3d.P/puro-CMV > CXCR4 > IRES/eGFP and pLV.EX2d.P/Neo-CMV > eGFP were successfully constructed, and the full-lengths of the two plasmids were determined to be 10,299 bp (CXCR4 sequence was between 2,569 and 3,649 bp) and 8,820 bp, respectively, using the automated DNA-sequencing instrument (Fig. 1A). The 293FT cells were co-transfected using the liposome method and the multinucleated cells (syncytia), which showed green fluorescence under the fluorescence microscope, were clearly visible at Day 2 after transfection (Fig. 1B). The titers of lenti-mCXCR4-eGFP/puro and lenti-eGFP/neo were 8.7×10^7 and 9.1×10^7 TU/ml, respectively. The infected BMSCs were selected with puromycin (for CXCR4-BMSCs) or neomycin (for null-BMSCs), and the noninfected BMSCs were completely necrosed after 3 or 4 days. The CXCR4-BMSCs (carrying both CXCR4 and eGFP genes) and null-BMSCs (carrying only eGFP gene) were obtained for further use (Fig. 1C).

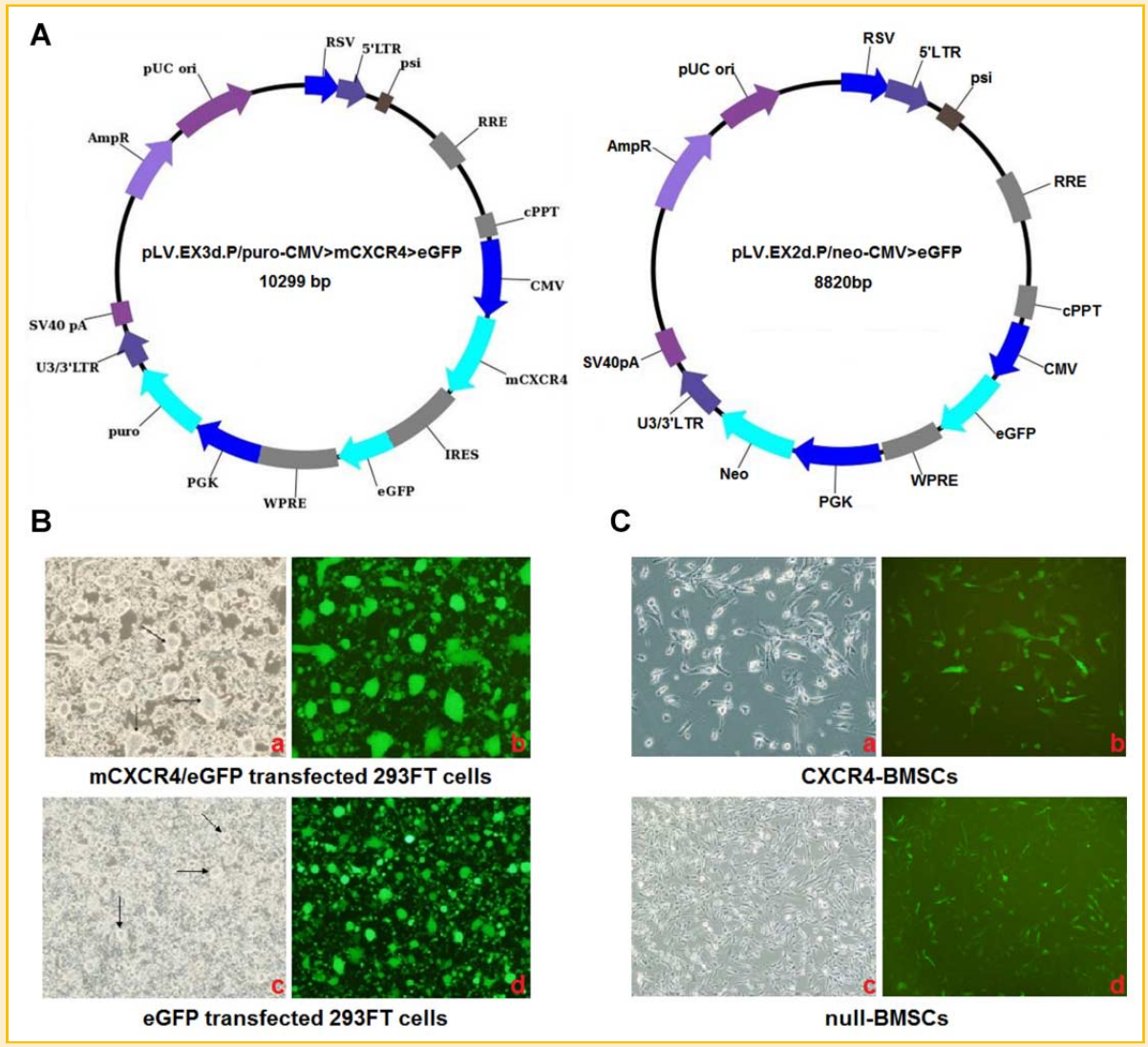

Fig. 1. Construction of CXCR4-BMSCs and null-BMSCs. A: Diagram of pLV.EX3d.P/puro-CMV > CXCR4 > IRES/eGFP *and* pLV.EX2d.P/Neo-CMV > eGFP. B: Morphology of the transfected 293FT cells at 2 days after transfection. 293FT cells were fused together and became multinucleated (syncytia; indicated by arrows; ×100) and green fluorescence in the lesion cells was observed under the fluorescence microscope (×100). C: Infected BMSCs after drug selection. a,b: CXCR4-BMSCs after 4 days of puromycin selection (×200); c,d: null-BMSCs after 3 days of neomycin selection (×100). The noninfected BMSCs were necrosed after drug selection and green fluorescence represented the positive cells.

CHARACTERIZATIONS OF CXCR4-BMSCs AND NULL-BMSCs

The mRNA level and protein expression of CXCR4 were high in the CXCR4-BMSCs, but low or undetectable in the null-BMSCs (Fig. 2A, B). To examine expression of CXCR4 on the cell surface, flow cytometry was performed and it revealed that the proportion of CXCR4-positive cells was significantly higher in the CXCR4-BMSCs (Fig. 2C). A series of analyses were performed to verify whether the infected cells still could exhibit the BMSC characteristics. The results indicated that the CXCR4-BMSCs and null-BMSCs both expressed high levels of the BMSC marker CD44 but were also negative for the hematopoietic marker CD45 (Fig. 3A). When being cultured in the different induction mediums, these cells could also be induced to undergo osteogenic, chondrogenic, and adipogenic differentiation (Fig. 3B). In addition, the viability of these cells was not changed and their proliferation ability was identical to that of the BMSCs (Fig. 3C).

SDF-1 PROTEIN EXPRESSION IN THE RENAL TISSUE AFTER AKI

The quantitative level of the SDF-1 protein expression relative to that of β-actin was illustrated in Figure 4A. We found that the sham-operated renal tissue exhibited a weak expression of SDF-1. However, after AKI, the SDF-1 protein expression was significantly increased and reached a maximal peak by 7 days, which was maintained for at least 14 days in the injured area.

BMSC MIGRATION TO THE RENAL TISSUE AFTER AKI

The BMSCs, CXCR4-BMSCs, and null-BMSCs were all labeled by BrdU. IHC analysis indicated that the BrdU-labeled ($BrdU^+$) BMSCs

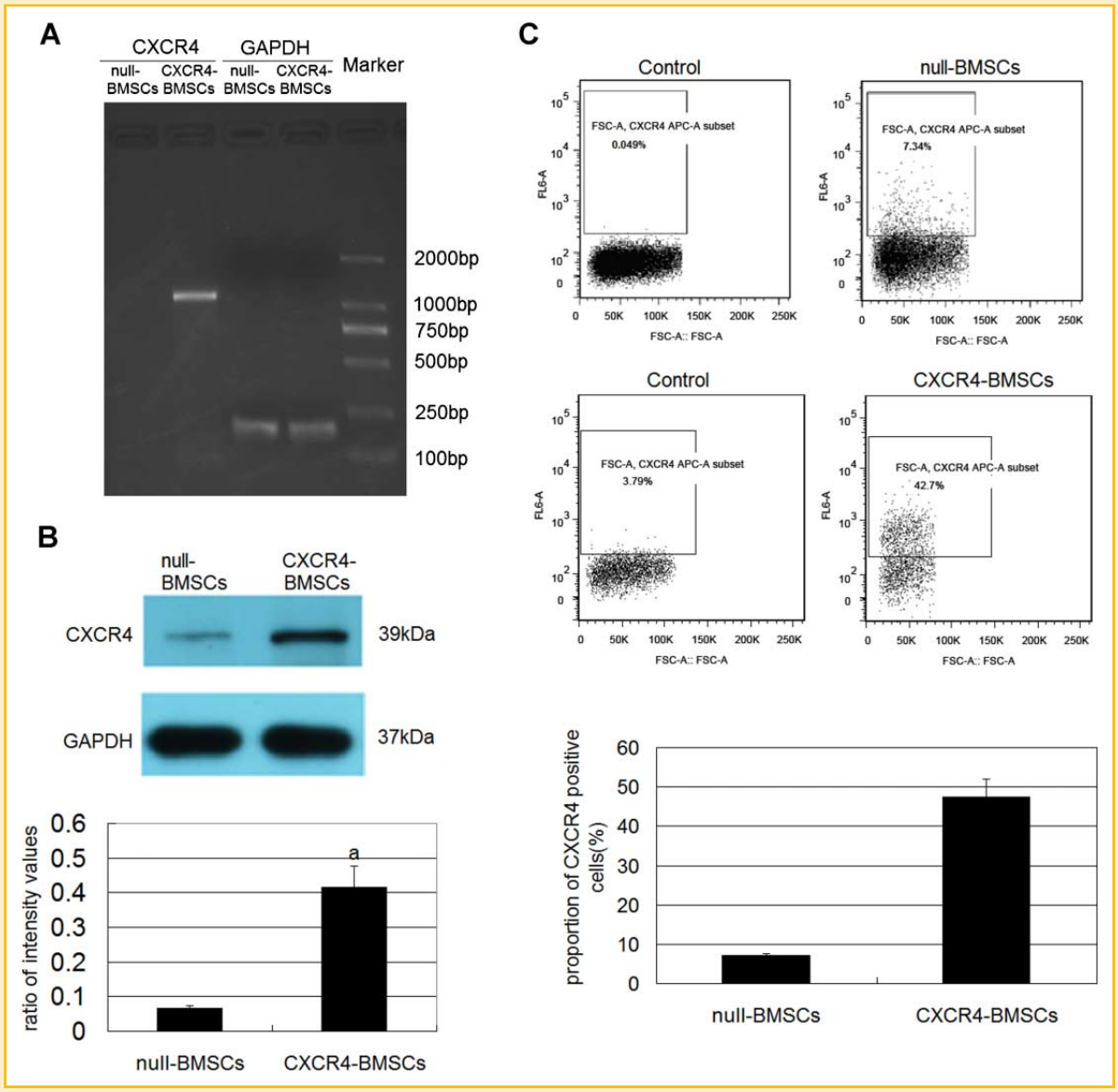

Fig. 2. CXCR4 levels for the transfected BMSCs. A: RT-PCR was used for the analysis of CXCR4 mRNA level in BMSCs. The mRNA level of GAPDH was used as the internal reference. B: Western blot analysis was performed to detect CXCR4 protein expression. The protein level of GAPDH was used as the internal reference. C: The cell surface expression of CXCR4 (% cells) was determined by flow cytometry. The results were presented as means ± standard deviation (SD). $^{a}P < 0.05$, compared to the null-BMSCs.

showed brown round nucleus (Fig. 4B). Some cells in the renal tissue of the AKI mice showed a brown nucleus in the BMSCs group, indicating that the $BrdU^{+}$ BMSCs migrated to the renal tissue. The proportion of $BrdU^{+}$ cells in the null-BMSCs group was similar to that in the BMSCs group. However, the CXCR4-BMSCs transplantation further increased the proportion of $BrdU^{+}$ BMSCs in the renal tissue, especially at Day 3 and Day 7 (Fig. 4C).

BLOOD BIOCHEMICAL INDICATORS AND ATN SCORING

Compared to those of the normal group, the levels of BUN and Scr and the ATN scoring of the model group mice were significantly increased after the surgery, reaching the peak at 1 day, followed by a declining trend (Fig. 4D and E). After BMSC transplantation, the levels of these indicators was decreased and showed significant differences at 3 days and 7 days (Fig. 4D,E). No differences were observed between the null-BMSCs group and the BMSCs group. However, after CXCR4-BMSC transplantation, the levels of BUN and Scr and the ATN scoring were sharply decreased, and were significantly lower than those of the BMSCs group at 7 and 14 days (Fig. 4D,E). In addition, the levels of BUN and Scr were close to those of the normal group at 14 days after transplantation (Fig. 4D).

SDF-1 LEVELS IN RTECs OR HR-RTECs

Western blot and ELISA analysis showed that the HR pretreatment significantly enhanced the SDF-1 protein expression in the RTECs and in the culture supernatant (Fig. 5A,B).

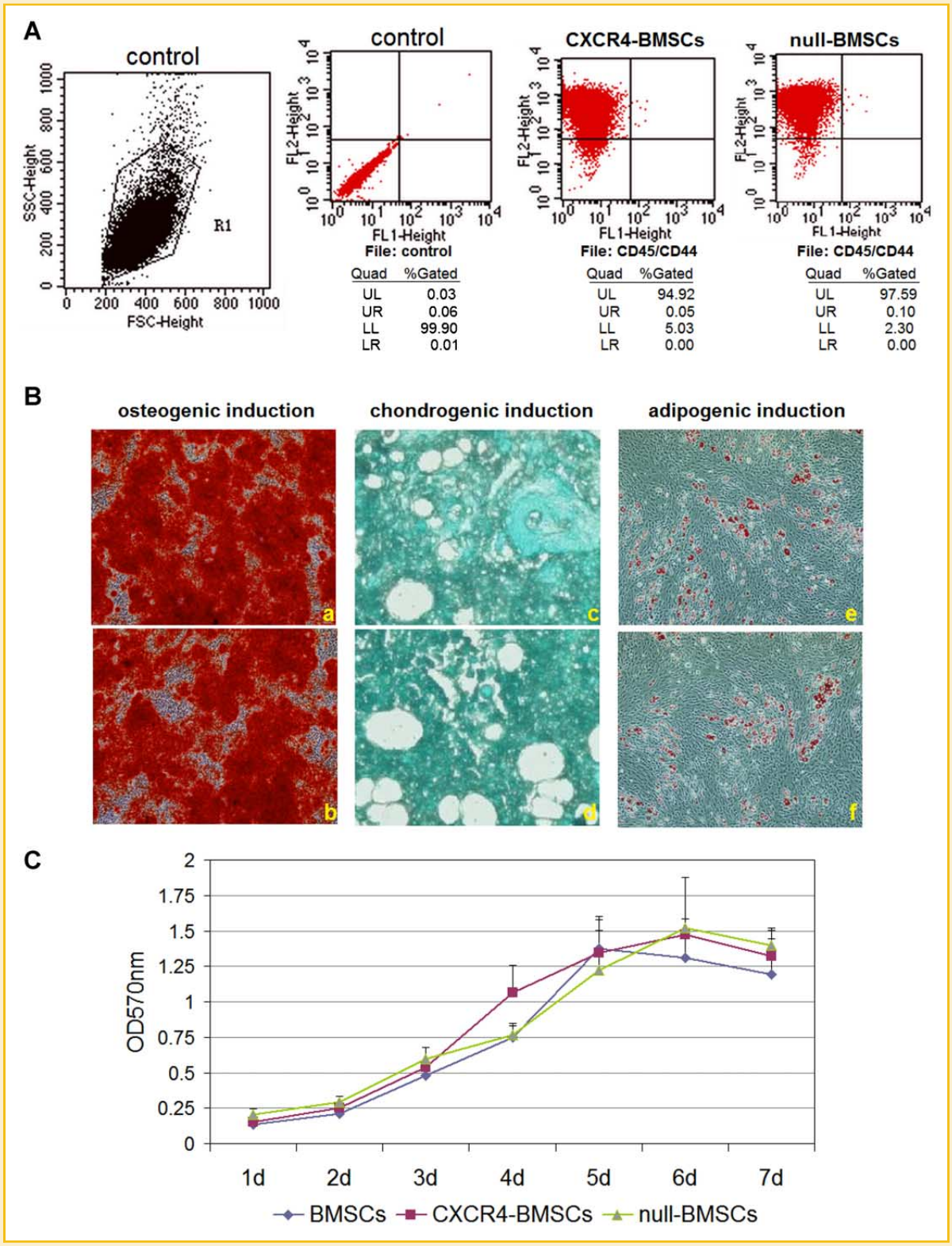

Fig. 3. Characterization of CXCR4-BMSCs and null-BMSCs. A: Flow cytometric analysis of CD44 and CD45 expression on the surface of BMSCs. B: Multi-directional differentiation potential. CXCR4-BMSCs (a,c,e), null-BMSCs (b,d,f). Calcium nodules were formed after osteogenic induction and showed red after alizarin red staining (a,b). After osteogenic induction, the blue in the alcian blue staining indicated the synthesis of proteoglycans by chondrocytes (c,d). The lipid precipitation showed in the oil red O staining represented adipogenic differentiation (e,f). C: Cell viability. No proliferative differences were observed among the BMSCs, CXCR4-BMSCs, and null-BMSCs. The results were presented as means ± SD.

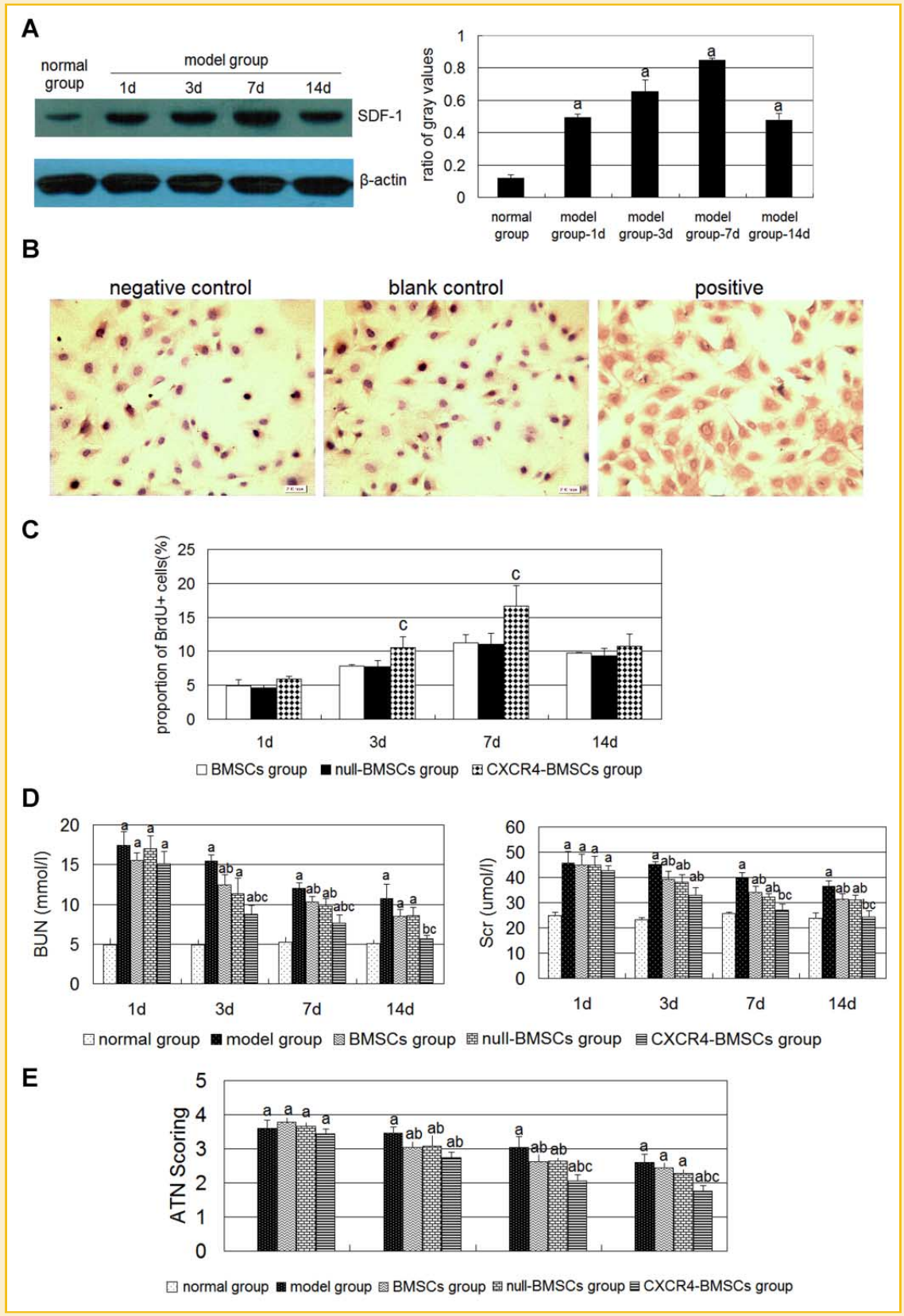

Fig. 4. Results of in vivo experiments. A: SDF-1 protein expression in the renal tissue after AKI or sham operation determined by Western blot. B: BrdU-labeled BMSCs (×200). BrdU-positive ($BrdU^+$) cells showed brown round nucleus. C: Quantitative analysis showed that the proportion of $BrdU^+$ cells in the CXCR4-BMSCs group was higher. D,E: The blood biochemical indicators and ATN scoring of each group. The ATN score of the normal group was zero, so it overlapped the abscissa. The results were presented as means ± SD. n = 5/group/time point. $^aP < 0.05$, compared to that of the normal group; $^bP < 0.05$, compared to that of the model group; $^cP < 0.05$, compared to that of the BMSCs group.

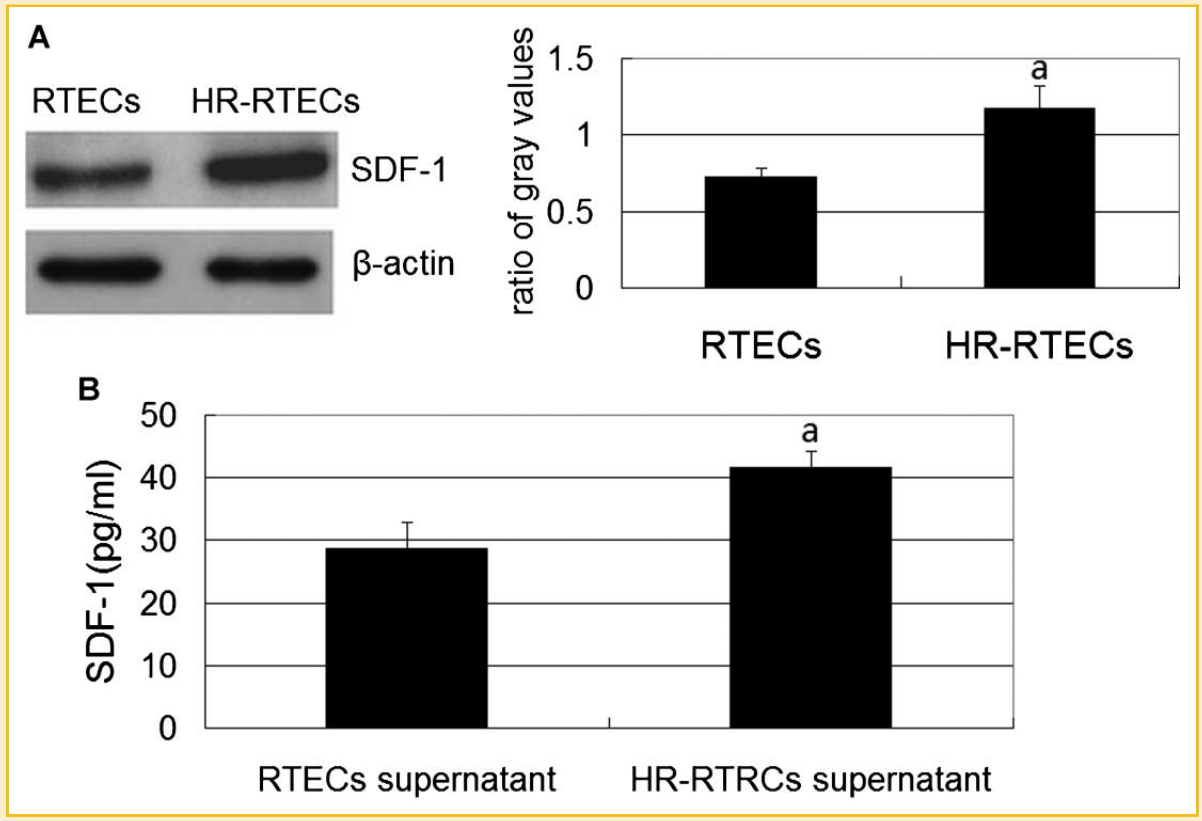

Fig. 5. SDF-1 levels. A: SDF-1 protein expression inside the cells. B: SDF-1 concentration in the supernatant of culture medium. The results were presented as means ± SD. Six duplicate wells were set for each group. $^{a}P < 0.05$, compared to that of the RTECs (or the RTEC culture medium supernatant).

EFFECTS OF CXCR4 GENE MODIFICATION ON BMSC MIGRATION TO THE AKI MICROENVIRONMENT IN VITRO

After AKI, SDF-1 was rapidly induced in the injured renal tissue together with an increased accumulation of BMSCs. In addition, the increased expression of CXCR4 on the BMSC surface was consistent with the higher number of accumulated BMSCs in the injured renal tissue. We next asked if the SDF-1 level in the renal tissue and the CXCR4 expression on the BMSC surface were functionally relevant to the BMSC migration to the kidney area after AKI. A transwell chamber-based migration assay was established to quantitatively evaluate the BMSC migration in vitro. The lower chamber was loaded with RTECs (cultured under the normoxia condition for 24 h) or HR-RTECs (cultured under the hypoxia condition and the re-oxygenation condition, respectively, for 12 h), while the upper chamber was loaded with BMSCs. As shown in Figure 6B, compared with that of the B/R group, the number of migrating BMSCs was increased in the B/H group whose SDF-1 level in the lower chamber was increased. The null-BMSC migration failed to show any difference, but the increased CXCR4 expression affected the BMSC migration and the number of migrating CXCR4-BMSCs was the highest among these groups. However, the migration of BMSCs, CXCR4-BMSCs and null-BMSCs could all be abolished by the pericubation of cells with the CXCR4-specific antagonist AMD3100, and the migrating cell numbers were all decreased to the level of the B/R group (Fig. 6C). Therefore, these results documented that SDF-1/CXCR4 had a significant effect on BMSC migration and that the increased CXCR4 expression on the BMSC surface could increase the migration of BMSCs to the AKI microenvironment.

PI3K/Akt AND MAPK ARE INVOLVED IN CXCR4-BMSC MIGRATION

To explore whether the increased CXCR4 expression enhanced the BMSC migration through the PI3K/Akt-dependent or MAPK-dependent pathways or both, we investigated the effects of LY294002 (PI3K/Akt inhibitor) and PD98059 (MAPK inhibitor) on the CXCR4-BMSC migration. As shown in Figure 6D and E, the separate treatment with the two inhibitors significantly attenuated the CXCR4-BMSC migration; however, the number of migrating cells was still significantly higher than that in the presence of AMD3100. However, the migrating number of cells in the presence of the both LY294002 and PD98059 showed no difference from that of the C/H + AMD3100 group (Fig. 6F). These results indicated that both of the PI3K/Akt-dependent and MAPK-dependent signaling pathways were involved in the CXCR4-BMSC migration and each one played a partial role. Western blot analysis (Fig. 7A,B) also showed that the levels of both phospho-Akt and phospho-MAPK were increased in the BMSCs co-cultured with HR-RTECs, and reached the maximal peak in the CXCR4-BMSCs. However, their expression in the BSMCs, CXCR4-BMSCs, and null-BMSCs all returned to the basal level after pericubation with AMD3100.

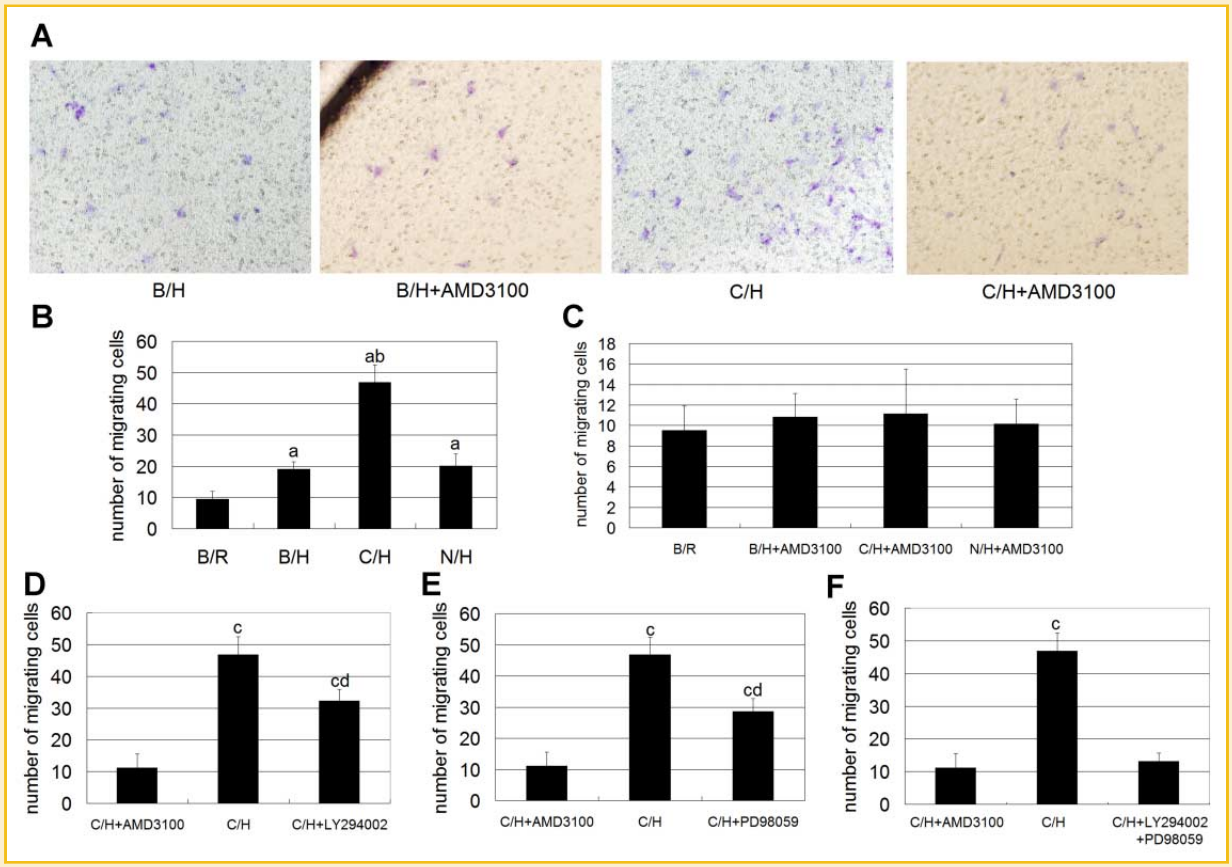

Fig. 6. BMSC migration in vitro. Chemotaxis assays of BMSCs were performed using the transwell chamber system. The transwell chambers were inserted into the 6-well plates cultured with RTECs (cultured under the normoxia condition for 24 h) or HR-RTECs (cultured under the hypoxia condition and the re-oxygenation condition, respectively, for 12 h), and mouse BMSCs, CXCR4-BMSCs and null-BMSCs were placed in the upper chambers. A: Images of the BMSCs migrating to the lower chamber under the microscope (×200). B: B/R (the B/R group: BMSCs in the upper chamber and RTECs in the lower chamber); B/H (the B/H group: BMSCs in the upper chamber and HR-RTECs in the lower chamber); C/H (the C/H group: CXCR4-BMSCs in the upper chamber and HR-RTECs in the lower chamber); N/H (the N/H group: null-BMSCs in the upper chamber and HR-RTECs in the lower chamber). Migration of BMSCs to the HR-RTECs culturing chamber was increased, and reached the maximal peak in the CXCR4-BMSCs. C: The BMSCs, CXCR4-BMSCs and null-BMSCs were all pre-incubated with a CXCR4-specific antagonist, AMD3100, for 30 min and then added into the upper chamber for the migration assay. AMD3100 totally blocked the cell migration. D,E: The CXCR4-BMSCs were pre-incubated with the PI3K inhibitor (LY294002) or MAPK inhibitor (PD98059) for 30 min and then added into the upper chamber for the migration assay. LY294002 and PD98059 both partly blocked the CXCR4-BMSC migration. F: The CXCR4-BMSCs were pre-incubated with LY294002 and PD98059 together for 30 min and then added into the upper chamber for the migration assay. The migrating number showed no difference from that in the C/H + AMD3100 group. The results were presented as means ± SD. Six duplicate wells were set for each group. $^{a}P < 0.05$, compared to that of the B/R group; $^{b}P < 0.05$, compared to that of the B/H group; $^{c}P < 0.05$, compared to that of the C/H + AMD3100 group; $^{d}P < 0.05$, compared to that of the C/H group.

DISCUSSION

Previous studies have shown that exogenous BMSCs can migrate to the injured kidneys and participate in the AKI repair, but the migration efficiency is limited. In our experiment, we also found that the injected BMSCs migrated to the injured kidney, and the levels of BUN, Scr, and the ATN scoring decreased in the BMSCs group. However, these indicators were still higher than those in the normal group. In addition, the decreases became smaller with the extension of time.

Migration of transplanted cells to the injured tissue is the prerequisite of the cell-based therapies. As a result, it is vital to enhance the kidney-directional migration of the transplanted BMSCs for increasing the efficiency of AKI repair. BMSC migration may involve various chemokines, cyokines, and integrins. Among the chemokines and their corresponding receptors, the SDF-1/CXCR4 axis is the most extensively studied system [Floridi et al., 2003; Yamaguchi et al., 2003; Wynn et al., 2004]. SDF-1, a member of the CXC sub-family, is widely expressed in many organs, and the ischemia microenvironment in the injured tissues can up-regulate its expression [Askari et al., 2003; Tögel et al., 2005; Shen et al., 2007; Lai et al., 2008; Li et al., 2009]. The increased SDF-1 expression was also observed in our animal experiment. In addition, the SDF-1 levels in the HR-RTECs and the culture medium supernatant were both significantly enhanced. CXCR4, one of the specific receptors of SDF-1, is expressed both on the cell surface and in the inside of BMSCs [Wang et al., 2008], and in fact, it normally exists in the inside of BMSCs [Wynn et al., 2004; Wang et al., 2008]. The increased SDF-1 in the injured tissue can cause it to mobilize to the cell surface [Li et al., 2010]. This translocated surface CXCR4 binds to SDF-1 and directs the migration of BMSCs toward the injured tissue. However, the expression of CXCR4 in BMSCs will be greatly diminished during

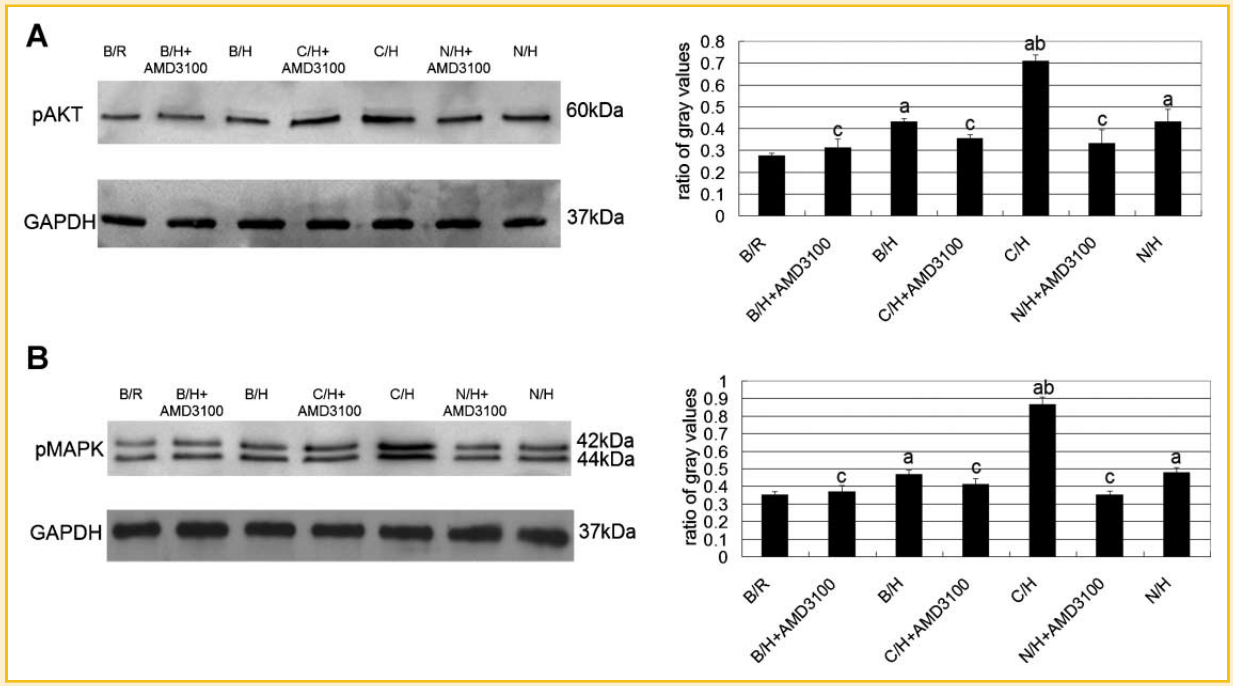

Fig. 7. Phosphorylation of AKT and MAPK in BMSCs. A: Phosphorylation of AKT and (B) Phosphorylation of MAPK. The levels of phospho-Akt and phospho-MAPK in the CXCR4-BMSCs co-cultured with the HR-RTECs reached the peak. AMD3100 blocked these phosphorylations. The results were presented as means ± SD. Six duplicate wells were set for each group. $^{a}P < 0.05$, compared to that of the B/R group; $^{b}P < 0.05$, compared to that of the B/H group; $^{c}P > 0.05$, compared to that of the B/R group.

the ex vivo expansion [Honczarenko et al., 2006; Karp and Leng Teo, 2009], which was also shown in the null-BMSCs in our experiment, and this will cause the mitigation of the chemotaxis effect of SDF-1 on BMSCs. Transplantation of stem cells over-expressing CXCR4 has shown significant protection against organ injury in other tissue repair models [Cheng et al., 2008; Park et al., 2011; Jones et al., 2012; Du et al., 2013], suggesting that enhancing the CXCR4 expression of BMSCs might have a potentially positive effect on their kidney-directional migration for AKI repair.

In our experiment, we enhanced the CXCR4 expression on the surface of BMSCs by gene transfection and used null-BMSCs as the control. The other characteristics of CXCR4-BMSCs and null-BMSCs, including the surface marker, differentiation potential, and cell viability, were not changed by gene transfection. Compared with null-BMSCs, CXCR4-BMSCs showed a remarkably enhanced expression of CXCR4. At the same time, the numbers of migrating CXCR4-BMSCs in our in vivo and in vitro experiments both were significantly increased. This stimulatory effect was also consistent with a greater improvement in renal function, including lower levels of BUN, Scr, and ATN scoring. In addition, the levels of BUN and Scr were even close to those of the normal group at 14 days after transplantation.

It is generally believed that SDF-1 mediates cell migration exclusively through its binding with CXCR4. However, CXCR7, another chemokine receptor, has also been shown to bind SDF-1 with high affinity [Burns et al., 2006]. Whereas, the ligand activation of CXCR7 by SDF-1 cannot cause cell migration [Liu et al., 2012]. In our study, we showed that the BMSC migration to the kidney area was mainly CXCR4-dependent, as confirmed by the increased migration of the CXCR4-BMSCs and its full inhibition by AMD3100, suggesting that CXCR7 may not be involved in the SDF-1-mediated migration of BMSCs. However, a study by Gheisari et al. [2012] showed that the overexpression of CXCR4 did not improve BMSCs homing. While the reasons for this disagreement with our observation are not completely known, we hypothesized that the BMSCs that they used likely experienced chromosomal abnormalities [Miura et al., 2006; Zhou et al., 2006] because of too much ex vivo expansion, or the mouse strain of BMSCs they used was more sensitive to the ex vivo expansion [Aguilar et al., 2007].

Both the PI3K/Akt and MAPK/ERK signal transduction pathways have been shown to mediate cell migration induced by chemokines or cytokines in different cell types [Dimmeler et al., 2001; Barbero et al., 2003; Ackah et al., 2005; Yu et al., 2010; Bobis-Wozowicz et al., 2011]. Previous studies on BMSC migration also have suggested that the activation of AKT and MAPK not only can increase the secretion of actin and myosin, which are related to BMSC movement, but they can also contribute to the secretion of matrix metalloproteinase (MMP) to degrade the extracellular matrix and basilar membrane, which is beneficial for BMSC migration [Kollet et al., 2003]. In our experiment, Western blot analysis showed that the levels of phospho-Akt and phospho-MAPK reached the maximal peak in the CXCR4-BMSCs and were restored to the basal level by AMD3100. The migration assays with PI3K-specific inhibitor (LY294002) and MAPK inhibitor (PD98059) showed that the separate treatment with both inhibitors significantly attenuated the migration of the CXCR4-BMSCs, however, the numbers remained higher than that in the C/H + AMD3100 group. Yet in the presence of both

inhibitors, the migrating number was similar to that of the C/H + AMD3100 group. Therefore, it is likely that both PI3K/Akt and MAPK/ERK transduction pathways are involved in the enhancement of BMSC migration induced by CXCR4 overexpression.

In conclusion, our study indicated that CXCR4 overexpression could enhance the migration of BMSCs to the kidney tissues after AKI along with the greater improvement in renal functions. The SDF-1/CXCR4 axis via the activation of PI3K/Akt and MAPK in the BMSCs could be the possible mechanisms. Therefore, CXCR4-BMSCs can be a better option for the cell transplantation therapy of AKI.

ACKNOWLEDGMENTS

We gratefully acknowledge the financial supports from Shanghai Rising-star Program (12QA1405000), Shanghai Municipal Natural Science Foundation (11ZR1449600), and Shanghai Key Projects of Basic Research (12DJ1400203).

REFERENCES

Ackah E, Yu J, Zoellner S, Iwakiri Y, Skurk C, Shibata R, Ouchi N, Easton RM, Galasso G, Birnbaum MJ, Walsh K, Sessa WC. 2005. Akt1/protein kinase Balpha is critical for ischemic and VEGF-mediated angiogenesis. J Clin Invest 115:2119–2127.

Aguilar S, Nye E, Chan J, Loebinger M, Spencer-Dene B, Fisk N, Stamp G, Bonnet D, Janes SM. 2007. Murine but not human mesenchymal stem cells generate osteosarcoma-like lesions in the lung. Stem Cells 25:1586–1594.

Askari AT, Unzek S, Popovic ZB, Goldman CK, Forudi F, Kiedrowski M, Rovner A, Ellis SG, Thomas JD, DiCorleto PE, Topol EJ, Penn MS. 2003. Effect of stromal-cell-derived factor 1 on stem-cell homing and tissue regeneration in ischaemic cardiomyopathy. Lancet 362:697–703.

Barbero S, Bonavia R, Bajetto A, Porcile C, Pirani P, Ravetti JL, Zona GL, Spaziante R, Florio T, Schettini G. 2003. Stromal cell-derived factor 1alpha stimulates human glioblastoma cell growth through the activation of both extracellular signal-regulated kinases 1/2 and Akt. Cancer Res 63:1969–1974.

Bobis-Wozowicz S, Miekus K, Wybieralska E, Jarocha D, Zawisz A, Madeja Z, Majka M. 2011. Genetically modified adipose tissue-derived mesenchymal stem cells overexpressing CXCR4 display increased motility, invasiveness, and homing to bone marrow of NOD/SCID mice. Exp Hematol 39:686–696.e4.

Burns JM, Summers BC, Wang Y, Melikian A, Berahovich R, Miao Z, Penfold MET, Sunshine MJ, Littman DR, Kuo CJ, Wei K, McMaster BE, Wright K, Howard MC, Schall TJ. 2006. A novel chemokine receptor for SDF-1 and I-TAC involved in cell survival, cell adhesion, and tumor development. J Exp Med 203:2201–2213.

Cheng Z, Ou L, Zhou X, Li F, Jia X, Zhang Y, Liu X, Li Y, Ward CA, Melo LG, Kong D. 2008. Targeted migration of mesenchymal stem cells modified with CXCR4 gene to infarcted myocardium improves cardiac performance. Mol Ther 16:571–579.

Dimmeler S, Aicher A, Vasa M, Mildner-Rihm C, Adler K, Tiemann M, Rütten H, Fichtlscherer S, Martin H, Zeiher AM. 2001. HMG-CoA reductase inhibitors (statins) increase endothelial progenitor cells via the PI 3-kinase/Akt pathway. J Clin Invest 108:391–397.

Du Z, Wei C, Yan J, Han B, Zhang M, Peng C, Liu Y. 2013. Mesenchymal stem cells overexpressing C-X-C chemokine receptor type 4 improve early liver regeneration of small-for-size liver grafts. Liver Transpl 19:215–225.

Eliopoulos N, Zhao J, Bouchentouf M, Forner K, Birman E, Yuan S, Boivin M-N, Martineau D. 2010. Human marrow-derived mesenchymal stromal cells decrease cisplatin renotoxicity in vitro and in vivo and enhance survival of mice post-intraperitoneal injection. Am J Physiol Renal Physiol 299:F1288–F1298.

Floridi F, Trettel F, Di Bartolomeo S, Ciotti MT, Limatola C. 2003. Signalling pathways involved in the chemotactic activity of CXCL12 in cultured rat cerebellar neurons and CHP100 neuroepithelioma cells. J Neuroimmunol 135:38–46.

Gatti S, Bruno S, Deregibus MC, Sordi A, Cantaluppi V, Tetta C, Camussi G. 2011. Microvesicles derived from human adult mesenchymal stem cells protect against ischaemia-reperfusion-induced acute and chronic kidney injury. Nephrol Dial Transplant 26:1474–1483.

Gheisari Y, Azadmanesh K, Ahmadbeigi N, Nassiri SM, Golestaneh AF, Naderi M, Vasei M, Arefian E, Mirab-Samiee S, Shafiee A, Soleimani M, Zeinali S. 2012. Genetic modification of mesenchymal stem cells to overexpress CXCR4 and CXCR7 does not improve the homing and therapeutic potentials of these cells in experimental acute kidney injury. Stem Cells Dev 21:2969–2980.

Herrera MB, Bussolati B, Bruno S, Fonsato V, Romanazzi GM, Camussi G. 2004. Mesenchymal stem cells contribute to the renal repair of acute tubular epithelial injury. Int J Mol Med 14:1035–1041.

Hoffmann J, Glassford AJ, Doyle TC, Robbins RC, Schrepfer S, Pelletier MP. 2010. Angiogenic effects despite limited cell survival of bone marrow-derived mesenchymal stem cells under ischemia. Thorac Cardiovasc Surg 58:136–142.

Honczarenko M, Le Y, Swierkowski M, Ghiran I, Glodek AM, Silberstein LE. 2006. Human bone marrow stromal cells express a distinct set of biologically functional chemokine receptors. Stem Cells 24:1030–1041.

Jones GN, Moschidou D, Lay K, Abdulrazzak H, Vanleene M, Shefelbine SJ, Polak J, De Coppi P, Fisk NM, Guillot PV. 2012. Upregulating CXCR4 in human fetal mesenchymal stem cells enhances engraftment and bone mechanics in a mouse model of osteogenesis imperfecta. Stem Cells Transl Med 1:70–78.

Karp JM, Leng Teo GS. 2009. Mesenchymal stem cell homing: The devil is in the details. Cell Stem Cell 4:206–216.

Kollet O, Shivtiel S, Chen Y-Q, Suriawinata J, Thung SN, Dabeva MD, Kahn J, Spiegel A, Dar A, Samira S, Goichberg P, Kalinkovich A, Arenzana-Seisdedos F, Nagler A, Hardan I, Revel M, Shafritz DA, Lapidot T. 2003. HGF, SDF-1, and MMP-9 are involved in stress-induced human CD34+ stem cell recruitment to the liver. J Clin Invest 112:160–169.

Lai P, Li T, Yang J, Xie C, Zhu X, Xie H, Ding X, Lin S, Tang S. 2008. Upregulation of stromal cell-derived factor 1 (SDF-1) expression in microvasculature endothelial cells in retinal ischemia-reperfusion injury. Graefes Arch Clin Exp Ophthalmol 246:1707–1713.

Li N, Lu X, Zhao X, Xiang F-L, Xenocostas A, Karmazyn M, Feng Q. 2009. Endothelial nitric oxide synthase promotes bone marrow stromal cell migration to the ischemic myocardium via upregulation of stromal cell-derived factor-1alpha. Stem Cells 27:961–970.

Li M, Yu J, Li Y, Li D, Yan D, Qu Z, Ruan Q. 2010. CXCR4 positive bone mesenchymal stem cells migrate to human endothelial cell stimulated by ox-LDL via SDF-1alpha/CXCR4 signaling axis. Exp Mol Pathol 88:250–255.

Liu N, Tian J, Wang W, Cheng J, Hu D, Zhang J. 2011. Effect and mechanism of erythropoietin on mesenchymal stem cell proliferation in vitro under the acute kidney injury microenvironment. Exp Biol Med (Maywood) 236:1093–1099.

Liu H, Liu S, Li Y, Wang X, Xue W, Ge G, Luo X. 2012. The role of SDF-1-CXCR4/CXCR7 axis in the therapeutic effects of hypoxia-preconditioned mesenchymal stem cells for renal ischemia/reperfusion injury. PLoS ONE 7: e34608.

Miura M, Miura Y, Padilla-Nash HM, Molinolo AA, Fu B, Patel V, Seo B-M, Sonoyama W, Zheng JJ, Baker CC, Chen W, Ried T, Shi S. 2006. Accumulated chromosomal instability in murine bone marrow mesenchymal stem cells leads to malignant transformation. Stem Cells 24:1095–1103.

Morigi M, Imberti B, Zoja C, Corna D, Tomasoni S, Abbate M, Rottoli D, Angioletti S, Benigni A, Perico N, Alison M, Remuzzi G. 2004. Mesenchymal stem cells are renotropic, helping to repair the kidney and improve function in acute renal failure. J Am Soc Nephrol 15:1794–1804.

Park SA, Ryu CH, Kim SM, Lim JY, Park SI, Jeong CH, Jun JA, Oh JH, Park SH, Oh W, Jeun S-S. 2011. CXCR4-transfected human umbilical cord blood-derived mesenchymal stem cells exhibit enhanced migratory capacity toward gliomas. Int J Oncol 38:97–103.

Semedo P, Wang PM, Andreucci TH, Cenedeze MA, Teixeira VPA, Reis MA, Pacheco-Silva A, Câmara NOS. 2007. Mesenchymal stem cells ameliorate tissue damages triggered by renal ischemia and reperfusion injury. Transplant Proc 39:421–423.

Shen LH, Li Y, Chen J, Zacharek A, Gao Q, Kapke A, Lu M, Raginski K, Vanguri P, Smith A, Chopp M. 2007. Therapeutic benefit of bone marrow stromal cells administered 1 month after stroke. J Cereb Blood Flow Metab 27:6–13.

Stolzing A, Scutt A. 2006. Effect of reduced culture temperature on antioxidant defences of mesenchymal stem cells. Free Radic Biol Med 41: 326–338.

Tögel F, Isaac J, Hu Z, Weiss K, Westenfelder C. 2005. Renal SDF-1 signals mobilization and homing of CXCR4-positive cells to the kidney after ischemic injury. Kidney Int 67:1772–1784.

Wang Y, Deng Y, Zhou GQ. 2008. SDF-1alpha/CXCR4-mediated migration of systemically transplanted bone marrow stromal cells towards ischemic brain lesion in a rat model. Brain Res 1195:104–112.

Wynn RF, Hart CA, Corradi-Perini C, O′Neill L, Evans CA, Wraith JE, Fairbairn LJ, Bellantuono I. 2004. A small proportion of mesenchymal stem cells strongly expresses functionally active CXCR4 receptor capable of promoting migration to bone marrow. Blood 104:2643–2645.

Yamaguchi J, Kusano KF, Masuo O, Kawamoto A, Silver M, Murasawa S, Bosch-Marce M, Masuda H, Losordo DW, Isner JM, Asahara T. 2003. Stromal cell-derived factor-1 effects on ex vivo expanded endothelial progenitor cell recruitment for ischemic neovascularization. Circulation 107:1322–1328.

Yu J, Li M, Qu Z, Yan D, Li D, Ruan Q. 2010. SDF-1/CXCR4-mediated migration of transplanted bone marrow stromal cells toward areas of heart myocardial infarction through activation of PI3K/Akt. J Cardiovasc Pharmacol 55:496–505.

Zhou YF, Bosch-Marce M, Okuyama H, Krishnamachary B, Kimura H, Zhang L, Huso DL, Semenza GL. 2006. Spontaneous transformation of cultured mouse bone marrow-derived stromal cells. Cancer Res 66:10849–10854.